

Towards microscopic resolution in holoscopy

Gesa Lilith Franke^{1,2}, Dierck Hillmann³, Christian Lührs³, Peter Koch³, Jörn Wollenzin³,
Gereon Hüttmann¹

¹Institute of Biomedical Optics, University of Lübeck, Germany

²Medical Laser Center Lübeck, Germany

³Thorlabs GmbH, Germany

ABSTRACT

Holoscopy is a new imaging approach combining digital holography and full-field Fourier-domain optical coherence tomography. The interference pattern between light scattered by a sample and a defined reference wave is recorded and processed numerically. During reconstruction numerical refocusing is applied, overcoming the limitation of the focal depth and thus a uniform, diffraction limited lateral resolution over the whole measurement depth can be obtained. The advantage of numerical refocusing becomes especially significant for imaging at high numerical apertures (NAs). We use a high-resolution setup based on a Mach-Zehnder interferometer with an high-resolution microscope objective (NA = 0.75). For reliable reconstruction of a sample volume the Rayleigh length of the microscope objective and the axial resolution, given by the spectral range of the light source, need to be matched. For a 0.75 NA objective a tunable light source with a sweeping range of ~ 300 nm is required. Here we present as a first step a tunable Ti:sapphire laser with a tuning range of 187 nm. By characterizing the spectral properties of the Ti:sapphire laser and determining the axial point spread function we demonstrate the feasibility of this light source for high-resolution holoscopy.

Keywords: optical coherence tomography, digital holography, holoscopy, optical coherence microscopy, tomography, microscopy

1. INTRODUCTION

In Fourier-domain optical coherence tomography (FD-OCT) the lateral and axial resolutions are decoupled. The axial resolution is constant over the whole imaging depth and is defined by the center wavelength and the spectral width which is covered by the light source. The lateral resolution is defined by the optics that images the backscattered light from the sample onto the detector. According to Gaussian optics, lateral resolution and depth of focus are connected and both are defined by the numerical aperture (NA) of the imaging system. While the lateral resolution in the focal plane increases with NA, the focal depth (described by the Rayleigh length) decreases. In confocal imaging of scanned OCT out-of-focus photons are rejected before detection. In full-field (FF-) FD-OCT^{1,2} photons from all depths are detected, but the degraded lateral resolution outside the focal plane causes blurred images. This effect was demonstrated by imaging point scatterers – particles with a size below the lateral resolution – as shown in Fig. 1a. Here a polyurethane resin, doped with red iron oxide particles (particle size: 300 – 800 nm),³ was imaged with a full-field FD-OCT setup at low NA (0.05).

Holoscopy is a new imaging approach combining digital holography (DH) and FF-FD-OCT.^{4,5} As in FF-FD-OCT photons are detected from all depths but imaging with optimal resolution is not limited to twice the Rayleigh length. By applying virtual refocusing mechanisms as in DH a diffraction limited depth-independent lateral resolution is provided over the whole penetration depth. This advantage of holoscopy is already visible at quite low NA when imaging point scatterers (Fig. 1b) but becomes even more significant when going to higher lateral resolutions. In most other optical imaging techniques z -scanning is inevitable for measuring a high resolution tomographic volume of a sample. In high-resolution holoscopy imaging of deep volumes is possible without

Further author information:

G.F.: E-mail: franke@bmo.uni-luebeck.de, Telephone: +49 (0) 451 500 6510

D.H.: E-mail: dhillmann@thorlabs.de, Telephone: +49 (0) 451 2903 256

G.H.: E-mail: huettmann@bmo.uni-luebeck.de, Telephone: +49 (0) 451 500 6530

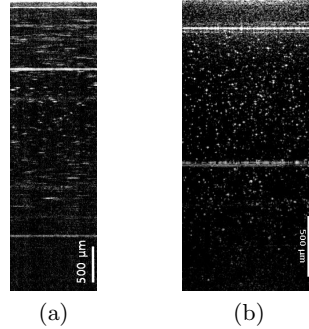


Figure 1: B-scans of a phantom with scattering nano particles acting as point scatterers, imaged with an NA of 0.05. a) Full-field FD-OCT shows a high sensitivity outside the focus region due to the lack of a confocal gating. The lateral resolution degrades significantly outside the Rayleigh length. b) Hologscopy shows constant resolution and sensitivity over the complete measurement depth.

z-scanning. However, to get a good image quality the lateral resolution of the imaging and the axial resolution of the FF-FD-OCT need to be matched. This requires for microscopic resolution an ultra-broadband tunable light source.

2. RECONSTRUCTION

Hologscopy combines elements from FD-OCT and DH to obtain diffraction limited lateral resolution over the whole imaging depth. As in DH the light field of a reflecting sample is detected. This is done in an interferometric setup by recording the interference pattern of the sample light field with a known reference wave by an area detector – a so-called hologram. When implementing an off-axis reference beam a spatial carrier frequency separates the signal term from its complex conjugated term, DC parts and autocorrelation signals of the hologram.⁶ The signal term can be selected by applying a two-dimensional filter in the Fourier domain. After an inverse Fourier transform a complex hologram without DC parts and without complex conjugated image is achieved. The filtered hologram is multiplied with a reconstruction wave, obtained from the known reference wave. A subsequent numerical back propagation of the sample light field into a plane inside the sample is applied and a sharp image of the chosen layer is obtained. One method for propagating a light wave is the angular spectrum approach, where each hologram is decomposed into plane waves and each plane wave is then propagated independently. Finally the plane waves are re-superimposed and provide the image data.⁶ This works well for three-dimensional surfaces and very low scattering samples, but when applied to scattering samples, the light fields of all scatterers superimpose. This results in sharp and blurred images being overlaid and thus in a loss of the sample information. In hologscopy multiple holograms are recorded during the sweep of a tunable light source. The reconstruction process is applied to each hologram, where the respective wavelength is used for reconstruction; all wave fields are propagated to the same layer within the sample. A one-dimensional Fourier transform is applied along the wave number axis – with suitable re-sampling if the sweep is non-linear in k – and gives the specific depth information for each scatterer within the sample. For constant lateral resolution over depth the procedure can be repeated with different reconstruction depths and thus different numerical foci. By stitching the sharp layers from all reconstructions together a constant, diffraction limited resolution can be achieved in the whole volume.

3. HIGH RESOLUTION SETUP

Hologscopy measurements can be performed with holographic setups for reflective samples. In most cases a holographic setup consists of a interferometer with a monochromatic long coherent light source. With an area detector the amplitude and phase of the light field backscattered by the sample, which are encoded in the fringe pattern of the interference signal between sample and reference light, are recorded. By implementing imaging optics for magnification of the fringe pattern high-resolution measurements can be performed.^{6,7} In Hologscopy the monochromatic light source is replaced by a tunable laser. A schematic setup for a high-resolution configuration can be seen in Fig. 2. In this Mach-Zehnder based setup the sample is illuminated with a collimated beam

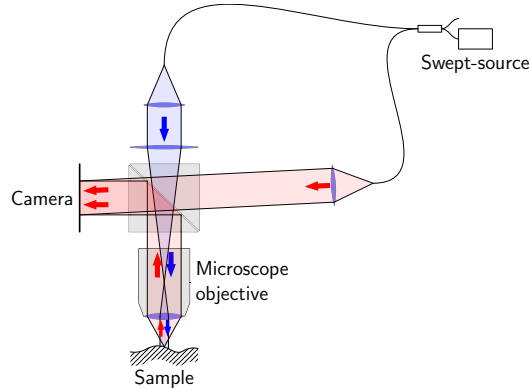


Figure 2: Mach-Zehnder configuration for high-resolution measurements with a microscope objective in the sample arm.

via an achromatic lens and a microscope objective. The backscattered light fields of the scatterers within the sample are collimated by a high NA microscope objective before reaching the camera. The reference beam is a collimated beam which incidents with an angle of $\sim 2^\circ$ degree onto the camera. The separation of the image from autocorrelated and DC parts, as well as the complex conjugated image reduces artefacts due to reflexes from within the setup. The lateral resolution of this setup is determined by the NA of the microscope objective, as long as the interference pattern can be sampled correctly. The setup was implemented with a microscope objective with an NA of 0.75 ($40\times$ Zeiss Achromplan, working distance = 2.1 mm, water immersion). This NA corresponds to a Gaussian lateral resolution of $2w_0 = 0.71 \mu\text{m}$ and a Rayleigh length of $2z_R = 1.22 \mu\text{m}$ in water. The diameter of the collimated reference wave was 16 mm. It was superimposed with the backscattered light of the sample on a monochromatic CMOS camera (Mikrotron EoSens MC3010, 1680×1680 pixel, acquisition speed of 285 frames/s, pixel size $\Delta x = 8 \mu\text{m}$).

4. IMPLEMENTATION OF A RAPIDLY TUNABLE TI:SAPPHIRE LASER

For successful measurements with the introduced high-resolution setup, the axial resolution – defined by the tuning range of the light source – needs to be similar to the Rayleigh length of the microscope objective. For the introduced Rayleigh length of $2z_R = 1.22 \mu\text{m}$ a tuning range of approximately 300 nm needs to be provided for water immersion measurements when apodizing the spectrum rectangularly. Since there are no rapidly tunable light sources with this tuning range commercially available, we modified an manual tunable Ti:sapphire laser (Spectra-Physics 3900S) for fast automatic tuning by turning the Lyot filter by a galvanometric scanner. The laser was pumped with a 4.5 W pump laser (Spectra-Physics Millennia Vs). The tuning range of the Ti:sapphire was approximately 300 nm using a broadband chirped mirror set. Tuning rates up to 10 Hz were obtained. For characterizing the sweep quality of the laser the output intensity was coupled into one arm of a simple Michelson interferometer with almost identical arm lengths ($\Delta z \approx 400 \mu\text{m}$). The interference signal from both arms was detected via a photodiode. The galvanometric scanner was driven by a linear voltage ramp resulting in a linear change of the wavelength. Data acquisition was synchronized to the galvanometric driver voltage. For one sweep 1024 data points were acquired. The resulting modulated spectrum can be seen in Fig. 3a. The recorded spectrum was Hilbert transformed to obtain the imaginary part of the analytic signal. The phase of the complex signal contains the spectral phase information ϕ at each data point. The phase was unwrapped and converted into the corresponding wavelength λ . The resulting data array (Fig. 3b) was used for interpolation of the spectrum intensity to obtain a dechirped spectrum with data points being equidistant in the wavenumber k . With the derivative of the unwrapped spectral phase phase jumps during the sweep could be detected with high sensitivity. The derivative of a spectral phase with no severe phase jumps can be seen in Fig. 3c. The corresponding A-scan – derived from Fourier transforming the dechirped spectrum after Hann windowing – shows a good signal quality (Fig. 3d). Phase jumps during the sweep are caused by vibrations within the setup or misaligned position and angle of the birefringent filter in the resonator and can be seen in Fig. 3e. The corresponding A-scan (Fig. 3f) shows severe image artefacts as an increased noise level and additional broadend side lobes. At the present stage,

monitoring the spectral phase is inevitable while performing measurements. For sweeps with no severe phase jumps the Ti:sapphire laser can be used as tunable light source for full-field FD-OCT and holoscopy since the depth axis is the slow axis in those systems.

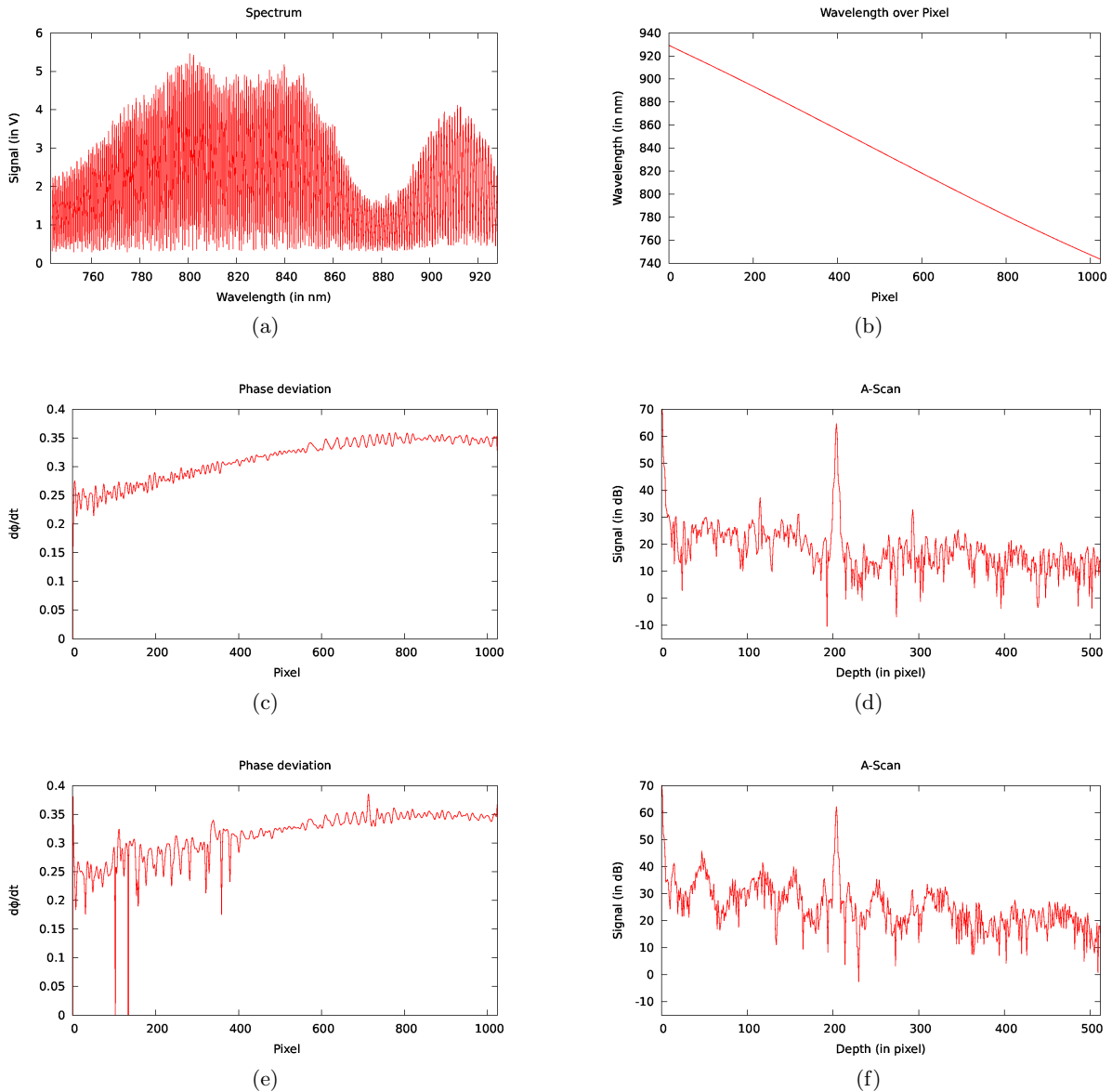


Figure 3: a) Recording of an interference signal during a wavelength scan of a Ti-sapphire laser. b) The phase information for each recorded pixel was converted to the wavelength at the specific acquisition time. c) The derivative of the phase information detects the change of the spectral phase during the sweep with high sensitivity. d) A-scan obtained from a spectrum with only slight phase jumps as shown in c) provides a sufficient image quality. e) Severe phase jumps caused by vibrations and misalignment of the Lyot filter. f) Corresponding A-scan shows severe artefacts with increased noise floor and several side lobes.

5. RESULTS

To determine the axial resolution of a setup using the tunable Ti:sapphire laser a surface of a wedge with 4 percent reflection was recorded and the measured data were reconstructed with the introduced algorithm. In addition to correct the dechirped spectrum, a numerical dispersion correction using calibration measurements as described in⁸ was applied to the data before processing. The reconstructed peak signal of the reflecting surface was used to determine the axial point spread function (PSF) of the setup. With a polynomial fit of second degree to the data points in the peak region the full width at half maximum (FWHM) was determined $4.7 \mu\text{m}$. This was 20 percent higher than the diffraction limited case.

With a commercially available light source, the Superlum Broadcaster (BS 840-HR), an axial FWHM of

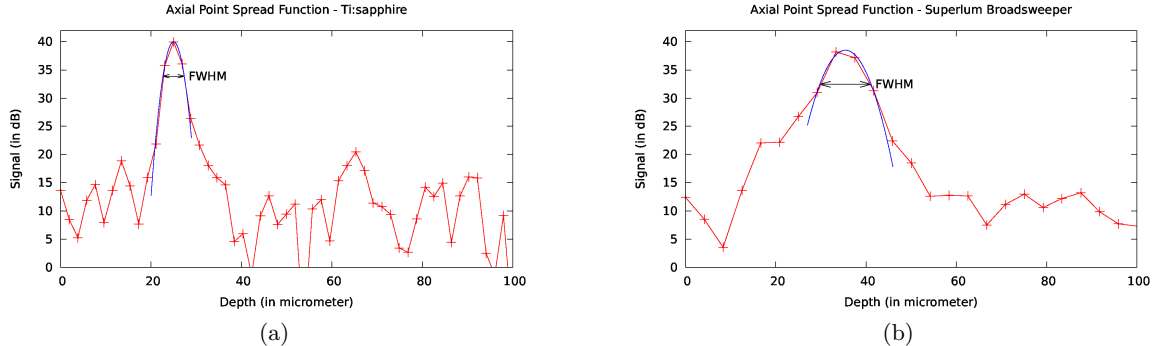


Figure 4: The axial point spread function determined by the FWHM ($= -6 \text{ dB}$) of the peak of a reflecting surface for the Ti:sapphire laser (a) and the Superlum Broadcaster (b)

$11.34 \mu\text{m}$, 35 percent above the diffraction limit, was achieved. The Broadcaster is a well-characterized, phase-stable light source with a center wavelength of $\lambda_0 = 841 \text{ nm}$ and a spectral width of $\Delta\lambda = 82 \text{ nm}$. Both axial point spread functions are slightly above the ideal pixel width for a Hann shaped signal.⁹ This can be explained by the non-rectangular shape of the spectrum before Hann windowing and residual non-compensated dispersion.

6. DISCUSSION AND OUTLOOK

We have introduced a holoscopy setup with so far unreached lateral resolution. To provide microscopic resolution in three dimensions the axial resolution has to match the Rayleigh length of the magnifying imaging optics. We have demonstrated a Ti:sapphire laser with an automated tuning mechanism by rotating a birefringent filter in the resonator using a galvanometric scanner. The spectral properties of the wavelength sweep allow for FF-FD-OCT and holoscopy. Monitoring the spectral phase to avoid severe phase jumps during the sweep is inevitable. So far a tuning range of 187 nm has been implemented. To obtain an almost isotropic resolution with the introduced high-resolution setup the tuning range needs to be further increased to $\sim 300 \text{ nm}$.

Aberrations are induced by the microscope objective, that significantly destroy the image quality for refocusing

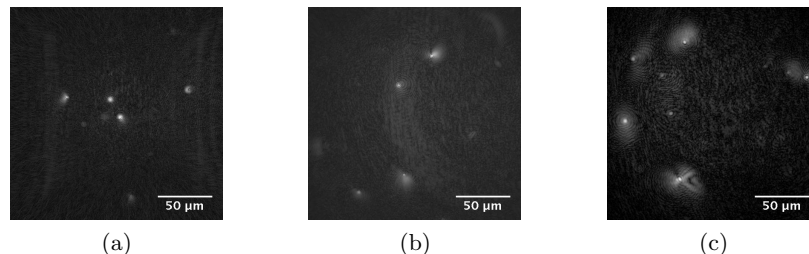


Figure 5: When using high NA microscope objectives in the holoscopy setup, aberrations occur outside the focal plane. While the effect is not severe very close to the focal plane (a), it becomes more and more significant when imaging outside the focal plane, as can be seen in b) for $\sim 45 \mu\text{m}$ and c) for $\sim 117 \mu\text{m}$ outside of focus.

to out-of-focus planes within a volume. While the objective is corrected for aberrations within the focal plane, the image quality is significantly reduced when obtaining image information outside the focal region (Fig. 5). Thus a numerical aberration correction is inevitable, when aiming for high-resolution holoscopy.

REFERENCES

- [1] Považay, B., Unterhuber, A., Hermann, B., Sattmann, H., Arthaber, H., and Drexler, W., “Full-field time-encoded frequency-domain optical coherence tomography,” *Opt. Express* **14**(17), 7661–7669 (2006).
- [2] Bonin, T., Franke, G., Hagen-Eggert, M., Koch, P., and Hüttmann, G., “In vivo Fourier-domain full-field OCT of the human retina with 1.5 million A-lines/s,” *Opt. Lett.* **35**(20), 3432–3434 (2010).
- [3] Woolliams, P. D., Ferguson, R. A., Hart, C., Grimwood, A., and Tomlins, P. H., “Spatially deconvolved optical coherence tomography,” *Appl Opt* **49**(11), 2014–21 (2010).
- [4] Hillmann, D., Lührs, C., Bonin, T., Koch, P., and Hüttmann, G., “Holoscopy—holographic optical coherence tomography,” *Opt. Lett.* **36**(13), 2390–2392 (2011).
- [5] Hillmann, D., Franke, G., Lührs, C., Koch, P., and Hüttmann, G., “Efficient holoscopy image reconstruction,” *Optics Express* **20**(19), 21247–21263 (2012).
- [6] Kim, M. K., “Principles and techniques of digital holographic microscopy,” *SPIE Reviews* **1**(1), 018005 (2010).
- [7] Schnars, U. and Jueptner, W., [*Digital holography*], Springer (2005).
- [8] Makita, S., Fabritius, T., and Yasuno, Y., “Full-range, high-speed, high-resolution 1- μ m spectral-domain optical coherence tomography using BM-scan for volumetric imaging of the human posterior eye,” *Optics express* **16**(12), 8406–8420 (2008).
- [9] Harris, F. J., “On the use of windows for harmonic analysis with the discrete Fourier transform,” *Proceedings of the IEEE* **66**(1), 51–83 (1978).